JCTC Journal of Chemical Theory and Computation

Article

Cite This: J. Chem. Theory Comput. 2019, 15, 2925−2932

pubs.acs.org/JCTC

Vertex Corrections to the Polarizability Do Not Improve the *GW* Approximation for the Ionization Potential of Molecules

Alan M. Lewis[†] and Timothy C. Berkelbach*[,‡,§]

[†]Department of Chemistry and James Franck Institute, University of Chicago, Chicago, Illinois 60637, United States

[‡]Department of Chemistry, Columbia University, New York, New York 10027, United States

[§]Center for Computational Quantum Physics, Flatiron Institute, New York, New York 10010, United States

ABSTRACT: The *GW* approximation is based on the neglect of vertex corrections, which appear in the exact self-energy and the exact polarizability. Here, we investigate the importance of vertex corrections in the polarizability only. We calculate the polarizability with equation-of-motion coupled-cluster theory with single and double excitations (EOM-CCSD), which rigorously includes a large class of diagrammatically defined vertex corrections beyond the random phase approximation (RPA). As is well-known, the frequency-dependent polarizability predicted by EOM-CCSD is quite different and generally more accurate than that predicted by the RPA. We evaluate the effect of these vertex corrections on a test set of 20 atoms and molecules. When using a Hartree−Fock reference, ionization potentials predicted by the *GW* approximation with the RPA polarizability are typically overestimated with a mean absolute error of 0.3 eV. However, those predicted with a vertex-corrected polarizability are typically underestimated with an increased mean absolute error of 0.5 eV. This result suggests that vertex corrections in the self-energy cannot be neglected, at least for molecules. We also assess the behavior of eigenvalue self-consistency in vertex-corrected *GW* calculations, finding a further worsening of the predicted ionization potentials.

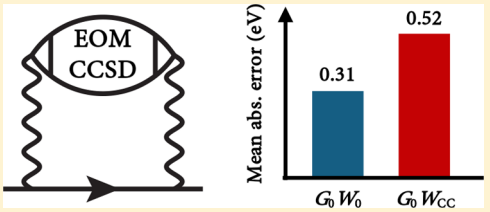

1. INTRODUCTION

The *GW* approximation[1] has been widely and successfully used to calculate the charged excitation energies associated with electron addition and removal. It has been applied to a variety of solids, including simple metals, semiconductors, and transition metal oxides,[1−10] and more recently to atoms and molecules.[9,11−19] Since its introduction, a number of attempts have been made to improve upon the *GW* approximation through the inclusion of diagrammatically defined vertex corrections beyond the random phase approximation (RPA). In some cases, vertex corrections are found to improve the accuracy of predicted excitation energies.[20−23] However, in other cases, the lowest-order vertex corrections produce results that are only marginally different, in both the condensed phase[24−29] and isolated molecules.[17,18,30]

Here, we implement a large class of infinite-order vertex corrections to the polarizability using equation-of-motion coupled-cluster theory with single and double excitations (EOM-CCSD). In addition to the particle−hole ring diagrams resummed by the RPA, EOM-CCSD includes particle−hole ladder diagrams, particle−particle ladder diagrams, exchange diagrams, and mixtures of all of the above. Furthermore, similar to the conventional *GW*-based implementation of the Bethe−Salpeter equation,[31,32] the propagator lines are dressed and particle−hole interactions are screened. We use this improved polarizability to construct a more accurate screened Coulomb interaction *W*, for use in the *GW* approximation; because this style of vertex corrections aims to calculate *W* in terms of the response of a test charge due to a test charge, it is sometimes referred to as G_0W^{tc-tc}. We assess this vertex-corrected *GW* approximation by calculating the ionization potentials of the 20 smallest atoms and molecules of the *GW*100 test set, which has recently been introduced for the purpose of benchmarking different implementations of the *GW* approximation.[15,16,18,19] By comparing our results to those obtained using conventional RPA screening, we conclude that vertex corrections to the polarizability worsen the accuracy of the *GW* approximation for ionization potentials of molecules. We also implement eigenvalue self-consistency in our vertex-corrected *GW* calculations and again find no improvement. We conclude that high-order vertex corrections to the structure of the self-energy are required to improve on existing methods.

2. THEORY

Charged excitation energies, associated with electron addition and removal, can be calculated by finding the poles of the one-particle Green's function

$$G(1, 2) = -i\langle\Psi_0|T[\psi^\dagger(1)\psi(2)|\Psi_0\rangle \quad (1)$$

Here $\psi^\dagger$ and ψ are field operators, the labels 1 and 2 indicate a set of position and time variables, i.e., $1 = (\mathbf{r}_1, t_1)$, T is the time-ordering operator, and $|\Psi_0\rangle$ is the ground state of the many-electron system. In practice, G is usually calculated via the self-energy Σ, defined by the Dyson equation

Received: October 2, 2018
Published: April 1, 2019

DOI: 10.1021/acs.jctc.8b00995
J. Chem. Theory Comput. 2019, 15, 2925−2932

$$G(1,2) = G_0(1,2) + \int G_0(4,2)\Sigma(3,4)G(1,3)\,\mathrm{d}(3)\,\mathrm{d}(4) \tag{2}$$

where G_0 is a noninteracting or mean-field Green's function. If G_0 is chosen to be the Hartree−Green's function, then the exact self-energy may be written as[1]

$$\Sigma(1,2) = i\int G(1,4)W(1,3)\Gamma(4,2,3)\,\mathrm{d}(3)\,\mathrm{d}(4) \tag{3}$$

where W is the screened Coulomb interaction and Γ is a three-point vertex function. The screened Coulomb interaction is given by

$$\begin{aligned} W(1,2) &= v(1,2) + \int v(4,2)\Pi^{\star}(3,4)W(1,3)\,\mathrm{d}(3)\,\mathrm{d}(4) \\ &= v(1,2) + \int v(4,2)\Pi(3,4)v(1,3)\,\mathrm{d}(3)\,\mathrm{d}(4) \end{aligned} \tag{4}$$

where $v(1,2) = |\mathbf{r}_1 - \mathbf{r}_2|^{-1}\delta(t_1 - t_2)$ is the usual Coulomb interaction. In the screened Coulomb interaction, $\Pi^{\star}$ and Π are the irreducible and reducible polarizabilities

$$\Pi^{\star}(1,2) = -i\int G(2,3)G(4,2)\Gamma(3,4,1)\,\mathrm{d}(3)\,\mathrm{d}(4) \tag{5}$$

$$\Pi(1,2) = -i\langle\Psi_0|T[\tilde{\rho}(1)\tilde{\rho}(2)|\Psi_0\rangle \tag{6}$$

where $\tilde{\rho} = \rho - \langle\Psi_0|\rho|\Psi_0\rangle$ and $\rho = \psi^{\dagger}\psi$. The three-point vertex function Γ appearing in eqs 3 and 5 is defined by

$$\begin{aligned} \Gamma(1,2,3) = \delta(1,2)\delta(1,3) + \int \frac{\delta\Sigma(1,2)}{\delta G(4,5)}G(4,6)G(7,5) \\ \times \Gamma(6,7,3)\,\mathrm{d}(4)\,\mathrm{d}(5)\,\mathrm{d}(6)\,\mathrm{d}(7) \end{aligned} \tag{7}$$

The conventional GW approximation follows by setting $\Gamma(1,2,3) = \delta(1,2)\delta(1,3)$, i.e., neglecting vertex corrections, leading to

$$\Sigma(1,2) \approx iG(1,2)W(1,2) \tag{8}$$

$$\Pi^{\star}(1,2) \approx -iG(2,1)G(1,2) \tag{9}$$

In practice, the GW approximation is commonly implemented without self-consistency, where G and W are evaluated in a one-shot manner on the basis of the mean-field starting point, leading to the so-called G_0W_0 approximation.

The exact *reducible* polarizability given in eq 6 has a Lehmann representation

$$\begin{aligned} \Pi(1,2) = -i\theta(t_1 - t_2)\sum_{n>0} \mathrm{e}^{-i\Omega_n(t_1-t_2)}\rho_n(\mathbf{r}_1)\rho_n^*(\mathbf{r}_2) \\ + (1 \leftrightarrow 2) \end{aligned} \tag{10}$$

where $\rho_n(\mathbf{r}) = \langle\Psi_0|\rho(\mathbf{r})|\Psi_n\rangle$ and $\Omega_n = E_n - E_0$. We note that the reducible polarizability is closely related to a certain time-ordering of the two-particle Green's function.[33] Separating the GW self-energy into its exchange and correlation components gives

$$\Sigma^{\mathrm{x}}(1,2) = iG(1,2)v(1,2) \tag{11a}$$

$$\Sigma^{\mathrm{c}}(1,2) = iG(1,2)\int v(4,2)\Pi(3,4)v(1,3)\,\mathrm{d}(3)\,\mathrm{d}(4) \tag{11b}$$

In a finite single-particle basis, the frequency dependence can be treated analytically such that the correlation component of the self-energy is given by

$$\begin{aligned} \Sigma^{\mathrm{c}}_{pq}(\omega) = \sum_{n>0}\left[\sum_i \frac{(pi|\rho_n^*)(\rho_n|iq)}{\omega - (\varepsilon_i - \Omega_n) - i\eta}\right. \\ \left. + \sum_a \frac{(pa|\rho_n)(\rho_n^*|aq)}{\omega - (\varepsilon_a + \Omega_n) + i\eta}\right] \end{aligned} \tag{12}$$

where

$$(pq|\rho_n) = \int \mathrm{d}\mathbf{r}_1\int \mathrm{d}\mathbf{r}_2\phi_p^*(\mathbf{r}_1)\phi_q(\mathbf{r}_1)|\mathbf{r}_1 - \mathbf{r}_2|^{-1}\rho_n(\mathbf{r}_2) \tag{13}$$

Here and throughout, we use indices i, j to denote orbitals that are occupied and a, b to denote orbitals that are unoccupied in the mean-field reference determinant. Equation 12 provides the formalism by which any theory of the polarizability can be employed in the GW approximation. For example, conventional RPA screening (no vertex corrections), as defined by eq 9, is recovered if the excitation energies Ω_n are obtained from the familiar eigenvalue problem[34]

$$\begin{pmatrix} \mathbf{A} & \mathbf{B} \\ -\mathbf{B}^* & -\mathbf{A}^* \end{pmatrix}\begin{pmatrix} \mathbf{X} \\ \mathbf{Y} \end{pmatrix} = \begin{pmatrix} \mathbf{X} \\ \mathbf{Y} \end{pmatrix}\mathbf{\Omega} \tag{14}$$

where

$$A_{ia,jb} = (\varepsilon_a - \varepsilon_i)\delta_{ab}\delta_{ij} + \langle ib|aj\rangle \tag{15a}$$

$$B_{ia,jb} = \langle ij|ab\rangle \tag{15b}$$

two-electron integrals are defined by

$$\langle pq|rs\rangle = \int \mathrm{d}\mathbf{r}_1\int \mathrm{d}\mathbf{r}_2\phi_p^*(\mathbf{r}_1)\phi_q^*(\mathbf{r}_2)|\mathbf{r}_1 - \mathbf{r}_2|^{-1}\phi_r(\mathbf{r}_1)\phi_s(\mathbf{r}_2) \tag{16}$$

and the transition moments $\rho_n(\mathbf{r})$ are given by

$$\rho_n(\mathbf{r}) = \sum_{ai}[X_{ia}^{(n)}\phi_a(\mathbf{r})\phi_i^*(\mathbf{r}) + Y_{ia}^{(n)}\phi_i(\mathbf{r})\phi_a^*(\mathbf{r})] \tag{17}$$

with the orthonormalization condition

$$\sum_{ai}\{[X_{ai}^{(m)}]^*X_{ai}^{(n)} - [Y_{ai}^{(m)}]^*Y_{ai}^{(n)}\} = \delta_{nm} \tag{18}$$

This flavor of RPA is sometimes referred to as "direct RPA" because it neglects the exchange integrals that would arise from antisymmetrization in eq 15. If the antisymmetrized integrals $\langle pq||rs\rangle \equiv \langle pq|rs\rangle - \langle pq|sr\rangle$ are maintained, then the screening is equivalent to time-dependent Hartree−Fock (TDHF). This level of theory was used to implement vertex corrections in the recent work of Maggio and Kresse,[18] which will also be tested here.

Here, we implement vertex corrections in the polarizability by using EOM-CCSD transition densities and excitation energies in eq 12. The formalism rigorously subsumes RPA screening (no vertex corrections) and TDHF screening. Briefly, EOM-CCSD excitation energies are defined as eigenvalues of the similarity-transformed $\bar{H} = e^{-T}He^{T} - E_{\mathrm{CCSD}}$ in the subspace of determinants that are singly and doubly excited with respect to a reference determinant $|\Phi\rangle$. The operator T creates single and double excitations, $T = \sum_{ai} t_i^a a_a^{\dagger}a_i + \frac{1}{4}\sum_{abij} t_{ij}^{ab}a_a^{\dagger}a_b^{\dagger}a_ja_i$, and the amplitudes are determined by the nonlinear system of equations $\langle\Phi_i^a|$

DOI: 10.1021/acs.jctc.8b00995
J. Chem. Theory Comput. 2019, 15, 2925−2932

$e^{-T}He^{T}|\Phi\rangle = 0$ and $\langle\Phi_{ij}^{ab}|e^{-T}He^{T}|\Phi\rangle = 0$. The right-hand eigenstates of H are then given by

$$|\Psi_0\rangle = e^{T}|\Phi\rangle \tag{19a}$$

$$|\Psi_n\rangle = \left[r_0 + \sum_{ai} r_i^a a_a^\dagger a_i + \frac{1}{4}\sum_{abij} r_{ij}^{ab} a_a^\dagger a_b^\dagger a_j a_i\right] e^{T}|\Phi\rangle \tag{19b}$$

and the left-hand eigenstates ($n \geq 0$) by

$$\langle\tilde{\Psi}_n| = \langle\Phi|\left[l_0 + \sum_{ai} l_a^i a_i^\dagger a_a + \frac{1}{4}\sum_{abij} l_{ab}^{ij} a_i^\dagger a_j^\dagger a_b a_a\right] e^{-T} \tag{20}$$

The transition densities follow naturally

$$\rho_n(\mathbf{r}) = \sum_{pq} \phi_p^*(\mathbf{r})\phi_q(\mathbf{r})\langle\tilde{\Psi}_0|a_p^\dagger a_q|\Psi_n\rangle \tag{21a}$$

$$\rho_n^*(\mathbf{r}) = \sum_{pq} \phi_p^*(\mathbf{r})\phi_q(\mathbf{r})\langle\tilde{\Psi}_n|a_p^\dagger a_q|\Psi_0\rangle \tag{21b}$$

for which analytic expressions can be simply obtained.[35]

EOM-CCSD is universally viewed as superior to the HF-based RPA for electronic excitation energies of molecules. For excited states that are well-described as single excitations, EOM-CCSD is accurate to about 0.1−0.3 eV,[36] whereas the HF-based RPA displays errors of 1 eV or more.[37] Improved results can be obtained with alternative choices of the mean-field reference, inclusion or exclusion of exchange, or in combination with time-dependent density functional theory.[30,37−39] In a more rigorous sense, the RPA can be derived as an approximation to EOM-CCSD, as recently discussed by one of us.[40] Diagrammatically, the EOM-CCSD polarizability resums all particle−hole ring diagrams (as in the RPA), as well as particle−particle, hole−hole, and particle−hole ladder diagrams, exchange diagrams, and mixtures of all of the above. These extra diagrams define the class of vertex corrections included in the polarizability beyond the RPA. When the RPA or EOM-CCSD polarizability is used in the non-self-consistent *GW* approximation, we will term the method the G_0W_0 or G_0W_{CC} approximation, respectively. In Figure 1, we show some example self-energy diagrams included with an EOM-CCSD polarizability and identify some that are included in various lower levels of theory.

3. RESULTS

In the results to follow, we study atoms and molecules from the *GW*100 test set.[15] Due to the relatively high computational cost of obtaining many highly excited states via EOM-CCSD, we only consider the smallest 20 atoms and molecules, using the polarized double-ζ def2SVP basis set.[41,42] Although we have not optimized the performance, the calculation of ionization potentials with EOM-CCSD vertex corrections in the polarizability can be performed in a manner that scales as N^7. By comparing results within a given basis set, our conclusions are largely free of basis set incompleteness error but numerical values should not be compared to experiment or to predictions in other basis sets. To give a rough sense of basis set completeness, previous G_0W_0 calculations have shown that IPs calculated in this basis set underestimate the complete basis set limit by about 0.3−0.5 eV.[13] We have performed the following calculations for the five smallest atoms and molecules in the larger def2-TZVPP basis set and find that our results and conclusions are unchanged. Where appropriate, we will also compare to previously published results in larger basis sets, which demonstrate that our general conclusions are robust. All calculations were performed with the PySCF software package.[43]

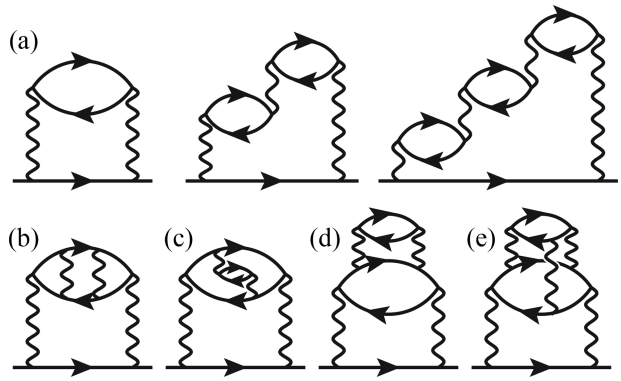

Figure 1. Example self-energy diagrams included when the polarizability is calculated with EOM-CCSD. The diagrams in part a are those included in the usual *GW* approximation with RPA screening. Diagram b is included with a TDHF polarizability, diagrams c and d would be included with a *GW*-based BSE polarizability, and diagram e—showing an example hole−hole ladder interaction—is only included with the EOM-CCSD polarizability.

First, to illustrate the differences between the RPA and EOM-CCSD polarizabilities, we consider the two-particle spectral function

$$C(\omega) = \sum_{n>0}\sum_{pq} |\langle\Psi_n|a_p^\dagger a_q|\Psi_0\rangle|^2 \delta(\omega - \Omega_n) \tag{22}$$

which is closely related to the imaginary part of the polarizability. This two-particle spectral function contains the same neutral-excitation quantities that enter into the *GW* self-energy, i.e., the transition density matrix elements and the excitation energies. In Figure 2, we show $C(\omega)$ for three example molecules, H_2 (for which EOM-CCSD is exact), H_2O, and HCl, over a very wide spectral range. RPA and EOM-CCSD calculations are done with a Hartree−Fock (HF) reference; see below for further discussion of this choice. Due to the very slow decay of $(\omega - E)^{-1}$, the self-energy at a given frequency is affected by a very large number of neutral excitation energies, as can be inferred from eq 12. Indeed, truncating the number of neutral excitation energies retained in the polarizability can affect the ionization potentials (IPs) by anywhere from 0.1 to 1 eV.[44] For all molecules, the RPA spectra are shifted to higher energies by 10 eV or more. This behavior is because the RPA polarizability does not include the electron−hole ladder diagrams that are included in the EOM-CCSD polarizability. These ladder diagrams reduce the excitation energy of molecules and lead to bound exciton states in semiconductors.[31,32,45] The overestimation of excitation energies can be partially, but not systematically, alleviated by choosing a mean-field reference with a smaller gap. Compared to HF, essentially all flavors of density functional theory (DFT) satisfy this property, which explains the popularity of the DFT+RPA approach. Roughly speaking, a larger spectral gap in the polarizability will reduce the screening, such that the *GW* correction to HF is less effective and the IPs are too large, which is indeed observed in our G_0W_0@HF calculations. Because the EOM-CCSD polarizability has a smaller (more accurate) spectral gap, the

DOI: 10.1021/acs.jctc.8b00995
J. Chem. Theory Comput. 2019, 15, 2925−2932

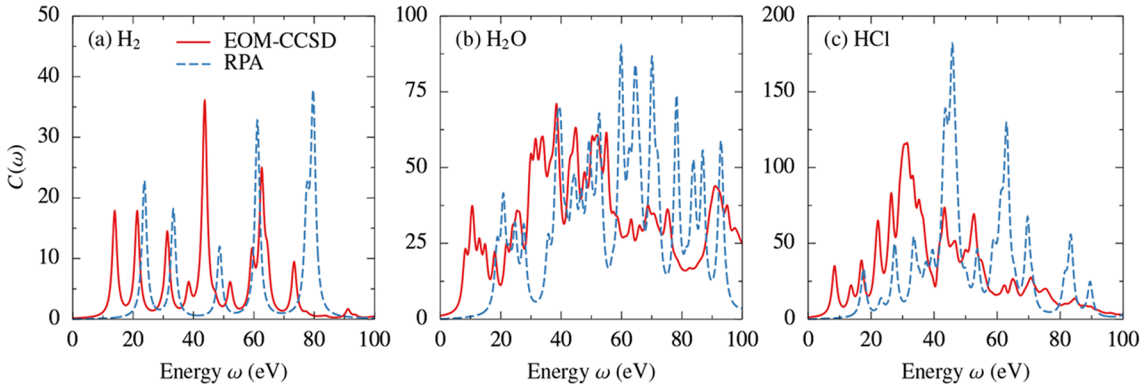

Figure 2. Spectral function of the polarizability $C(\omega)$ for H_2, H_2O, and HCl calculated using EOM-CCSD and the RPA. All calculations are done in the def2SVP basis using a Hartree−Fock reference and using a numerical broadening of 1 eV.

screening is stronger, the *GW* correction is larger, and the IPs are significantly reduced in magnitude.

In Table 1, we present the first IP of the 20 smallest atoms and molecules of the *GW*100 test set, obtained via G_0W_0 and G_0W_{CC}. As a reference, we calculate the first IP using ΔCCSD(T), i.e., as a difference in ground-state energies between the neutral and charged systems using CCSD with perturbative triple excitations. In all *GW* calculations, we use Hartree−Fock (HF) theory as the mean-field reference, which has been established as a good choice for molecules.[14,16,46] Importantly, the HF starting point has no self-interaction error through first order. However, the missing correlation and orbital relaxation leads to HF IPs that are too large in magnitude (orbital energies are too negative). Consistent with previous results,[16] the G_0W_0@HF approximation predicts reasonably accurate IPs, with a mean error (ME) of +0.19 eV and a mean absolute error (MAE) of 0.31 eV (these can be compared to identical calculations in the larger def2-TZVPP basis,[16] which have a ME of +0.26 eV and a MAE of 0.35 eV). The vertex-corrected G_0W_{CC}@HF approximation gives worse results and underestimates IPs, with a ME of −0.31 eV and a MAE of 0.52 eV. In particular, the vertex-corrected calculations give a less accurate IP for 11 of the 20 molecules. We also note that, for the two-electron molecules H_2 and He, the EOM-CCSD polarizability, and thus *W*, is exact; however, the results for both molecules are worse when the exact *W* is used in the *GW* approximation.

Table 1. First Ionization Potential in eV Calculated Using G_0W_0@HF, G_0W_{CC}@HF, and $G_{ev}W_{CC}$@HF, Where EOM-CCSD Is Used to Calculate the Screened Interaction W_{CC}[a]

molecule	ΔCCSD(T)	G_0W_0@HF	G_0W_{CC}@HF	$G_{ev}W_{CC}$@HF
He	24.31	24.32	23.82	23.78
Ne	21.08	20.98	20.32	20.19
H_2	16.26	16.24	15.97	15.99
Li_2	5.07	5.03	4.90	4.95
LiH	7.69	7.81	6.95	6.54
FH	15.60	15.64	14.99	14.82
Ar	15.20	15.31	15.06	15.00
H_2O	12.07	12.27	11.66	11.53
LiF	10.76	10.51	9.22	8.52
HCl	12.15	12.31	12.05	12.05
BeO	9.98	9.63	8.65	8.11
CO	13.70	14.73	14.11	13.97
N_2	15.27	16.98	16.69	16.68
CH_4	14.25	14.51	14.10	14.03
BH_3	13.17	13.42	13.03	12.98
NH_3	10.32	10.61	10.10	10.00
BF	10.82	10.98	10.69	10.70
BN	11.89	11.36	11.04	11.00
SH_2	9.89	10.07	9.81	9.82
F_2	15.56	16.03	15.30	15.02
ME		+0.19	−0.31	−0.44
MAE		0.31	0.52	0.64

[a]Errors are calculated with respect to ΔCCSD(T). All calculations are done in the def2SVP basis using a Hartree−Fock reference.

This reduction in the IP can be understood from Figure 3, which shows the frequency dependence of the real part of the self-energy for the highest occupied molecular orbital (HOMO), corresponding to the first IP. The poles of the self-energy with vertex corrections are clearly shifted to higher energies (less negative) by about 10 eV, consistent with the differences in the polarizabilities shown in Figure 2. The pole strengths are relatively unchanged, and therefore, the IPs are reduced in magnitude, compared to those predicted by the *GW* approximation without vertex corrections.

Although we do not show the detailed results here, we have also implemented vertex corrections at the TDHF level,[18] which can be viewed as intermediate between the RPA (no vertex corrections) and EOM-CCSD. TDHF vertex corrections to the polarizability add particle−hole ladder diagrams—shown in Figure 1b—that are responsible for excitonic effects and expected to be important in molecules. For the molecules considered here, the TDHF excitation energies are quite close to those of EOM-CCSD, such that the IPs predicted via the vertex-corrected *GW* approximation are similar. Specifically, the IPs predicted with TDHF vertex corrections exhibit a mean error of −0.28 eV and a mean absolute error of 0.50 eV. These can be compared to the analogous TDHF vertex-corrected results of ref 18 (there called $G_0W_0^{tc-tc}$), which have a ME of −0.06 eV and a MAE of 0.15 eV. Although these latter results appear more accurate than our own, the errors are obtained by comparing *GW* results extrapolated to the complete basis set limit to CCSD(T) results in a finite cc-pVQZ basis set; as discussed by those authors,[18] the CCSD(T) IPs are likely underestimated by 0.10−0.15 eV, such that a consistent comparison in the basis set limit would worsen the performance of those vertex-corrected *GW* calculations and

DOI: 10.1021/acs.jctc.8b00995
J. Chem. Theory Comput. 2019, 15, 2925−2932

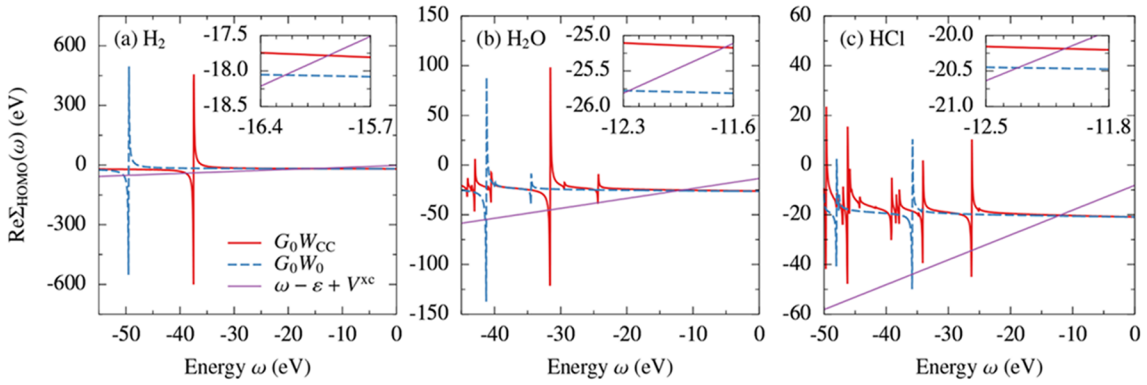

Figure 3. Real part of the HOMO self-energy for H_2, H_2O, and HCl calculated using the vertex-corrected G_0W_{CC} and non-vertex-corrected G_0W_0 approximations. Each inset magnifies a (0.7 eV) × (1 eV) region around the quasiparticle energies, where $\Sigma_{HOMO}(\omega) = \omega - \varepsilon + V^{xc}$. The self-energy is calculated with a small imaginary part of η = 0.03 eV.

bring them into better agreement with our own (for which errors are consistently calculated in the same basis set).

The *GW* self-energies calculated using the RPA, TDHF, and EOM-CCSD polarizabilities for the HCl molecule are shown in Figure 4. The similarity between the TDHF and EOM-CCSD polarizabilities can be understood on the basis of the weakly correlated nature of the molecules studied, as well as the dominant one-particle + one-hole nature of the low-energy excitations. For molecules or solid-state materials with a small or vanishing gap, the TDHF and EOM-CCSD polarizabilities are expected to differ more qualitatively and may yield larger differences in ionization potentials when used with the vertex-corrected *GW* approximation.

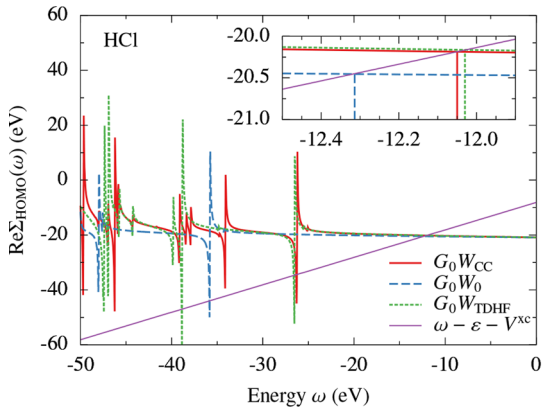

Figure 4. Same as in Figure 3c but also including the result with TDHF vertex corrections, corresponding to electron−hole interactions in the polarizability.

These collective results demonstrate that high-quality vertex corrections to the polarizability do not improve the ionization potentials of small molecules within the *GW* approximation; when used with a HF reference, these vertex corrections make the results worse by predicting IPs that are significantly too small in magnitude. However, we find that TDHF vertex corrections to the polarizability, as recently implemented by Maggio and Kresse[18] for both the polarizability and the self-energy, are a good approximation to those produced by the more expensive EOM-CCSD approach presented here and represent a promising and affordable approach for weakly correlated, gapped materials.

These findings can be compared to previous solid-state calculations, where it was found that adding low-order vertex corrections to the polarizability alone unphysically reduced the bandwidth[26] and increased the work function[47] of simple models of metals, and increased the quasiparticle energy of insulators and semiconductors.[27] It has also been shown that small improvements to the polarizability make little difference to the ionization potentials of atoms.[47] The present work extends these previous results by employing a far more accurate and diagrammatically defined polarizability, demonstrating the behavior across a range of molecular systems.

Having addressed the low-level RPA treatment of screening, we now mention the two remaining sources of error in the *GW* approximation: vertex corrections to the self-energy and self-consistency. The former are more challenging to implement than vertex corrections to the polarizability; however, future work will address this issue. While self-consistency is also challenging, one relatively inexpensive option is to enforce eigenvalue self-consistency.[5,48−53] In this approach, the quasiparticle eigenvalues associated with each orbital are replaced with the newly calculated quasiparticle energies after each iteration of the *GW* calculation until self-consistency is established. Despite not being fully self-consistent, these methods have been found to significantly reduce the starting point dependence of *GW* calculations.[50,52,53] Here, we implement and test eigenvalue self-consistency for EOM-CCSD vertex-corrected *GW* calculations.

A major advantage of using EOM-CCSD for vertex corrections is that the coupled-cluster framework is extremely insensitive to the choice of mean-field reference.[54] This can be understood by the Thouless theorem, which shows that the single excitation part of the coupled-cluster wave operator, e_1^T, is able to transform a Slater determinant into any other.[55] This insensitivity is responsible for the common choice of a HF reference, for which the working equations are simpler. In numerical tests, we find that eigenvalue self-consistency makes almost no change to the EOM-CCSD polarizability, and thus, we enforce eigenvalue self-consistency in *G* only (but the results should be understood as essentially those of complete eigenvalue self-consistency). We refer to this approach as $G_{ev}W_{CC}$; the IPs predicted by this method are listed in Table 1. We find that enforcing eigenvalue self-consistency further deterioriates the accuracy, yielding a mean error of −0.44 eV and a mean absolute error of 0.64 eV. We conclude that combining eigenvalue self-consistency with a large class of

DOI: 10.1021/acs.jctc.8b00995
J. Chem. Theory Comput. 2019, 15, 2925−2932

vertex corrections to the polarizability further worsens the *GW* approximation, leading to IPs that are severely underestimated in magnitude.

4. CONCLUSION

In this work, we have investigated the effect of high-quality vertex corrections to the polarizability for use in the *GW* approximation. Vertex corrections were implemented using EOM-CCSD, which corresponds to an infinite order resummation of particle−hole, particle−particle, and hole−hole ladder diagrams, in addition to the usual ring diagrams, and mixtures of all of the above.[40] The resulting polarizability is undeniably more accurate than that predicted by the RPA. However, the vertex-corrected *GW* approximation produces *worse* results than calculations without vertex corrections, when applied to a test set of 20 small atoms and molecules. Specifically, the improved treatment of screening correctly decreases the IPs; however, it overcompensates and predicts IPs that are significantly too small. Enforcing eigenvalue self-consistency also showed no improvement.

We have focused on the use of the *GW* approximation to predict the first IP, even though the Green's function contains much more information. It is possible that the vertex corrections implemented in the polarizability would yield an improvement in quantitites other than the principle IP. For example, it can be clearly seen in Figure 4 that different treatments of screening lead to very different structure in the self-energies at higher (more negative) energies, which will lead to significantly different predictions of the locations of satellite peaks in the one-particle spectral function. For example, in HCl, although the TDHF and EOM-CCSD vertex corrections predict very similar quasiparticle and first satellite peaks, they predict a second satellite peak that differs by about 5 eV. However, in all of the molecules we checked, the weight of these satellite peaks is so small so as to be physically inconsequential. It will be interesting to investigate the role of vertex corrections on the satellite structure of molecules or materials with stronger electron correlation.

As mentioned above, the only remaining approximation is the neglect of vertex corrections in the self-energy. Without these, the *GW* approximation neglects the transient interactions between the screened particle and the particle−hole pairs responsible for screening. Additionally, the neglected exchange diagrams in the self-energy are responsible for a self-screening error.[56,57] However, when the lowest-order vertex corrections to the self-energy were included in the calculation of the band gaps of silicon[58] and a semiconducting wire,[28] only small improvements were observed. Furthermore, these corrections are found to cancel with the lowest order corrections to the polarizability, as mentioned previously.[24−29] In order to systematically improve upon the G_0W_0 approximation, it appears necessary to include high-order vertex corrections to both the self-energy and the polarizability.

We note that a number of other Green's function based approaches include infinite-order vertex corrections in both the self-energy and the polarizability, including the two-particle−hole Tamm−Dancoff approximation,[59] the third-order algebraic diagrammatic construction (ADC(3)),[60] and the EOM-CC Green's function.[61,62] However, most of these methods do not provide the forward and backward time-orderings needed to entirely subsume the conventional RPA; two notable exceptions are the EOM-CC Green's function with single, double, and triple excitations, as discussed recently in relation to the *GW* approximation,[63] and the Faddeev random-phase approximation.[64,65]

AUTHOR INFORMATION

Corresponding Author

*E-mail: tim.berkelbach@gmail.com.

ORCID

Timothy C. Berkelbach: 0000-0002-7445-2136

Funding

This work was supported by the Air Force Office of Scientific Research under award number FA9550-18-1-0058.

Notes

The authors declare no competing financial interest.

ACKNOWLEDGMENTS

All calculations were performed with the PySCF software package,[43] using resources provided by the University of Chicago Research Computing Center. T.C.B. is an Alfred P. Sloan Research Fellow. The Flatiron Institute is a division of the Simons Foundation.

REFERENCES

(1) Hedin, L. New method for calculating the one-particle Green's function with application to the electron-gas-problem. *Phys. Rev.* **1965**, *139*, A796.

(2) Strinati, G.; Mattausch, H. J.; Hanke, W. Dynamical correlation effects on the quasiparticle bloch states of a covalent crystal. *Phys. Rev. Lett.* **1980**, *45*, 290−294.

(3) Strinati, G.; Mattausch, H. J.; Hanke, W. Dynamical aspects of correlation corrections in a covalent crystal. *Phys. Rev. B: Condens. Matter Mater. Phys.* **1982**, *25*, 2867.

(4) Hybertsen, M. S.; Louie, S. G. First-principles theory of quasiparticles: Calculation of band gaps in semiconductors and insulators. *Phys. Rev. Lett.* **1985**, *55*, 1418−1421.

(5) Hybertsen, M. S.; Louie, S. G. Electron correlation in semiconductors and insulators: Band gaps and quasiparticle energies. *Phys. Rev. B: Condens. Matter Mater. Phys.* **1986**, *34*, 5390−5413.

(6) Godby, R. W.; Schlüter, M.; Sham, L. J. Self-energy operators and exchange-correlation potentials in semiconductors. *Phys. Rev. B: Condens. Matter Mater. Phys.* **1988**, *37*, 10159−10175.

(7) Aryasetiawan, F.; Gunnarsson, O. The GW method. *Rep. Prog. Phys.* **1998**, *61*, 237.

(8) Aulbur, W. G.; Jönsson, L.; Wilkins, J. W. Quasiparticle Calculations in Solids. *Solid State Phys.* **2000**, *54*, 1−218.

(9) Hüser, F.; Olsen, T.; Thygesen, K. S. Quasiparticle GW calculations for solids, molecules, and two-dimensional materials. *Phys. Rev. B: Condens. Matter Mater. Phys.* **2013**, *87*, 1−14.

(10) Ergonenc, Z.; Kim, B.; Liu, P.; Kresse, G.; Franchini, C. Converged GW quasiparticle energies for transition metal oxide perovskites. *Phys. Rev. Mater.* **2018**, *2*, 24601.

(11) Rostgaard, C.; Jacobsen, K. W.; Thygesen, K. S. Fully self-consistent GW calculations for atoms and molecules. *Phys. Rev. B: Condens. Matter Mater. Phys.* **2010**, *81*, 85103.

(12) Bruneval, F. Ionization energy of atoms obtained from GW self-energy or from random phase approximation total energies. *J. Chem. Phys.* **2012**, *136*, 194107.

(13) van Setten, M. J.; Weigend, F.; Evers, F. The GW-Method for Quantum Chemistry Applications: Theory and Implementation. *J. Chem. Theory Comput.* **2013**, *9*, 232−246.

(14) Bruneval, F.; Marques, M. a. L. Benchmarking the starting points of the GW approximation for molecules. *J. Chem. Theory Comput.* **2013**, *9*, 324−329.

(15) Van Setten, M. J.; Caruso, F.; Sharifzadeh, S.; Ren, X.; Scheffler, M.; Liu, F.; Lischner, J.; Lin, L.; Deslippe, J. R.; Louie, S. G.; Yang, C.; Weigend, F.; Neaton, J. B.; Evers, F.; Rinke, P. GW100:

DOI: 10.1021/acs.jctc.8b00995
J. Chem. Theory Comput. 2019, 15, 2925−2932

Benchmarking G0W0 for Molecular Systems. *J. Chem. Theory Comput.* **2015**, *11*, 5665−5687.
(16) Caruso, F.; Dauth, M.; van Setten, M. J.; Rinke, P. Benchmark of GW Approaches for the GW100 Test Set. *J. Chem. Theory Comput.* **2016**, *12*, 5076.
(17) Hung, L.; Bruneval, F.; Baishya, K.; ÖÄŸüt, S. Benchmarking the GW Approximation and Bethe-Salpeter Equation for Groups IB and IIB Atoms and Monoxides. *J. Chem. Theory Comput.* **2017**, *13*, 2135−2146.
(18) Maggio, E.; Kresse, G. GW Vertex Corrected Calculations for Molecular Systems. *J. Chem. Theory Comput.* **2017**, *13*, 4765−4778.
(19) Govoni, M.; Galli, G. GW100: Comparison of Methods and Accuracy of Results Obtained with the WEST Code. *J. Chem. Theory Comput.* **2018**, *14*, 1895−1909.
(20) Shishkin, M.; Marsman, M.; Kresse, G. Accurate quasiparticle spectra from self-consistent GW calculations with vertex corrections. *Phys. Rev. Lett.* **2007**, *99*, 14−17.
(21) Grüneis, A.; Kresse, G.; Hinuma, Y.; Oba, F. Ionization potentials of solids: The importance of vertex corrections. *Phys. Rev. Lett.* **2014**, *112*, 096401.
(22) Chen, W.; Pasquarello, A. Accurate band gaps of extended systems via efficient vertex corrections in GW. *Phys. Rev. B: Condens. Matter Mater. Phys.* **2015**, *92*, 041115.
(23) Schmidt, P. S.; Patrick, C. E.; Thygesen, K. S. Simple vertex correction improves GW band energies of bulk and two-dimensional crystals. *Phys. Rev. B: Condens. Matter Mater. Phys.* **2017**, *96*, 205206.
(24) Rice, T. M. The effects of electron-electron interaction on the properties of metals. *Ann. Phys. (Amsterdam, Neth.)* **1965**, *31*, 100−129.
(25) Minnhagen, P. Vertex correction calculations for an electron gas. *J. Phys. C: Solid State Phys.* **1974**, *7*, 3013−3019.
(26) Mahan, G. D.; Sernelius, B. E. Electron-electron interactions and the bandwidth of metals. *Phys. Rev. Lett.* **1989**, *62*, 2718−2720.
(27) Del Sole, R.; Reining, L.; Godby, R. W. GWY approximation for electron self-energies in semiconductors and insulators. *Phys. Rev. B: Condens. Matter Mater. Phys.* **1994**, *49*, 8024−8028.
(28) de Groot, H.; Ummels, R.; Bobbert, P.; van Haeringen, W. Lowest-order corrections to the RPA polarizability and GW self-energy of a semiconducting wire. *Phys. Rev. B: Condens. Matter Mater. Phys.* **1996**, *54*, 2374−2380.
(29) Shirley, E. L. Self-consistent GW and higher-order calculations of electron states in metals. *Phys. Rev. B: Condens. Matter Mater. Phys.* **1996**, *54*, 7758−7764.
(30) Ma, H.; Govoni, M.; Gygi, F.; Galli, G. A Finite-field Approach for *GW* Calculations Beyond the Random Phase Approximation. *J. Chem. Theory Comput.* **2019**, *15*, 154−164.
(31) Rohlfing, M.; Louie, S. G. Electron-hole excitations and optical spectra from first principles. *Phys. Rev. B: Condens. Matter Mater. Phys.* **2000**, *62*, 4927−4944.
(32) Onida, G.; Reining, L.; Rubio, A. Electronic excitations: density-functional versus many-body Green's-function approaches. *Rev. Mod. Phys.* **2002**, *74*, 601−659.
(33) Fetter, A. L.; Walecka, J. D. *Quantum Theory of Many-Particle Systems*; Dover Publications: 2003.
(34) Ring, P.; Shuck, P. *The Nuclear Many-Body Problem*; Springer-Verlag: Berlin, Heidelberg, 1980.
(35) Stanton, J. F.; Bartlett, R. J. The equation of motion coupled-cluster method. A systematic biorthogonal approach to molecular excitation energies, transition probabilities, and excited state properties. *J. Chem. Phys.* **1993**, *98*, 7029.
(36) Schreiber, M.; Silva-Junior, M. R.; Sauer, S. P.; Thiel, W. Benchmarks for electronically excited states: CASPT2, CC2, CCSD, and CC3. *J. Chem. Phys.* **2008**, *128*, 134110.
(37) Wiberg, K. B.; De Oliveira, A. E.; Trucks, G. A comparison of the electronic transition energies for ethene, isobutene, formaldehyde, and acetone calculated using RPA, TDDFT, and EOM-CCSD. Effect of basis sets. *J. Phys. Chem. A* **2002**, *106*, 4192−4199.
(38) Sottile, F.; Bruneval, F.; Marinopoulos, A. G.; Dash, L. K.; Botti, S.; Olevano, V.; Vast, N.; Rubio, A.; Reining, L. TDDFT from molecules to solids: The role of long-range interactions. *Int. J. Quantum Chem.* **2005**, *102*, 684−701.
(39) Caricato, M.; Trucks, G. W.; Frisch, M. J.; Wiberg, K. B. Oscillator Strength: How Does TDDFT Compare to EOM-CCSD? *J. Chem. Theory Comput.* **2011**, *7*, 456−466.
(40) Berkelbach, T. C. Communication: Random-phase approximation excitation energies from approximate equation-of-motion coupled-cluster doubles. *J. Chem. Phys.* **2018**, *149*, 041103.
(41) Weigend, F.; Ahlrichs, R. Balanced basis sets of split valence, triple zeta valence and quadruple zeta valence quality for H to Rn: Design and assessment of accuracy. *Phys. Chem. Chem. Phys.* **2005**, *7*, 3297−3305.
(42) Weigend, F. Accurate Coulomb-fitting basis sets for H to Rn. *Phys. Chem. Chem. Phys.* **2006**, *8*, 1057−1065.
(43) Sun, Q.; Berkelbach, T. C.; Blunt, N. S.; Booth, G. H.; Guo, S.; Li, Z.; Liu, J.; McClain, J. D.; Sayfutyarova, E. R.; Sharma, S.; Wouters, S.; Chan, G. K. L. PySCF: the Python-based simulations of chemistry framework. *Wiley Interdiscip. Rev. Comput. Mol. Sci.* **2018**, *8*, No. e1340.
(44) Bruneval, F.; Rangel, T.; Hamed, S. M.; Shao, M.; Yang, C.; Neaton, J. B. MOLGW 1: Many-body perturbation theory software for atoms, molecules, and clusters. *Comput. Phys. Commun.* **2016**, *208*, 149−161.
(45) Hanke, W.; Sham, L. J. Local-field and excitonic effects in the optical spectrum of a covalent crystal. *Phys. Rev. B* **1975**, *12*, 4501.
(46) Caruso, F.; Rinke, P.; Ren, X.; Scheffler, M.; Rubio, A. Unified description of ground and excited states of finite systems: The self-consistent GW approach. *Phys. Rev. B: Condens. Matter Mater. Phys.* **2012**, *86*, 1−5.
(47) Morris, A. J.; Stankovski, M.; Delaney, K. T.; Rinke, P.; García-González, P.; Godby, R. W. Vertex corrections in localized and extended systems. *Phys. Rev. B: Condens. Matter Mater. Phys.* **2007**, *76*, 1−9.
(48) Pavlyukh, Y.; Hübner, W. Life-time of quasiparticle states in metallic clusters from GW theory. *Phys. Lett. A* **2004**, *327*, 241−246.
(49) Blase, X.; Attaccalite, C.; Olevano, V. First-principles GW calculations for fullerenes, porphyrins, phtalocyanine, and other molecules of interest for organic photovoltaic applications. *Phys. Rev. B: Condens. Matter Mater. Phys.* **2011**, *83*, 1−9.
(50) Faber, C.; Attaccalite, C.; Olevano, V.; Runge, E.; Blase, X. First-principles GW calculations for DNA and RNA nucleobases. *Phys. Rev. B: Condens. Matter Mater. Phys.* **2011**, *83*, 1−5.
(51) Marom, N.; Caruso, F.; Ren, X.; Hofmann, O. T.; Körzdörfer, T.; Chelikowsky, J. R.; Rubio, A.; Scheffler, M.; Rinke, P. Benchmark of GW methods for azabenzenes. *Phys. Rev. B: Condens. Matter Mater. Phys.* **2012**, *86*, 1−16.
(52) Kaplan, F.; Weigend, F.; Evers, F.; Van Setten, M. J. Off-diagonal self-energy terms and partially self-consistency in GW calculations for single molecules: Efficient implementation and quantitative effects on ionization potentials. *J. Chem. Theory Comput.* **2015**, *11*, 5152−5160.
(53) Kaplan, F.; Harding, M. E.; Seiler, C.; Weigend, F.; Evers, F.; Van Setten, M. J. Quasi-Particle Self-Consistent GW for Molecules. *J. Chem. Theory Comput.* **2016**, *12*, 2528−2541.
(54) Shavitt, I.; Bartlett, R. J. *Many-Body Methods in Chemistry and Physics: MBPT and Coupled-Cluster Theory*; Cambridge University Press: Cambridge, New York, 2009.
(55) Thouless, D. J. Stability conditions and nuclear rotations in the Hartree-Fock theory. *Nucl. Phys.* **1960**, *21*, 225−232.
(56) Romaniello, P.; Guyot, S.; Reining, L. The self-energy beyond GW: Local and nonlocal vertex corrections. *J. Chem. Phys.* **2009**, *131*, 154111.
(57) Wetherell, J.; Hodgson, M. J. P.; Godby, R. W. GW self-screening error and its correction using a local density functional. *Phys. Rev. B: Condens. Matter Mater. Phys.* **2018**, *97*, 121102.
(58) Bobbert, P. A.; Van Haeringen, W. Lowest-order vertex-correction contribution to the direct gap of silicon. *Phys. Rev. B: Condens. Matter Mater. Phys.* **1994**, *49*, 10326−10331.

DOI: 10.1021/acs.jctc.8b00995
J. Chem. Theory Comput. 2019, 15, 2925−2932

(59) Walter, O.; Schirmer, J. The two-particle-hole Tamm-Dancoff approximation (2ph-TDA) for atoms. *J. Phys. B: At. Mol. Phys.* **1981**, *14*, 3805.
(60) Schirmer, J.; Cederbaum, L. S.; Walter, O. New approach to the one-particle Green's function for finite Fermi systems. *Phys. Rev. A: At., Mol., Opt. Phys.* **1983**, *28*, 1237−1259.
(61) Nooijen, M.; Snijders, J. G. Coupled cluster approach to the single-particle Green's function. *Int. J. Quantum Chem.* **1992**, *44*, 55−83.
(62) Nooijen, M.; Snijders, J. G. Coupled cluster Green's function method: Working equations and applications. *Int. J. Quantum Chem.* **1993**, *48*, 15−48.
(63) Lange, M. F.; Berkelbach, T. C. On the Relation Between Equation-of-Motion Coupled-Cluster Theory and the GW Approximation. *J. Chem. Theory Comput.* **2018**, *14*, 4224.
(64) Barbieri, C.; Van Neck, D.; Dickhoff, W. H. Quasiparticles in neon using the Faddeev random-phase approximation. *Phys. Rev. A: At., Mol., Opt. Phys.* **2007**, *76*, 1−12.
(65) Degroote, M.; Van Neck, D.; Barbieri, C. Faddeev random-phase approximation for molecules. *Phys. Rev. A: At., Mol., Opt. Phys.* **2011**, *83*, 042517.

DOI: 10.1021/acs.jctc.8b00995
J. Chem. Theory Comput. 2019, 15, 2925−2932